Mapping smallholder maize farm distribution using multi-temporal Sentinel-1 data integrated with Sentinel-2, DEM and CHIRPS precipitation data in Google Earth Engine

Colette de Villiers[1,2], Cilence Munghemezulu[2,3], Solomon G. Tesfamichael[3] , Zinhle Mashaba-Munghemezulu[2] and George J. Chirima[1,2]
[1]Department of Geography, Geoinformatics and Meteorology, University of Pretoria, South Africa; email: colettedev007@gmail.com
[2]Geoinformation Science Division, Agricultural Research Council Institute for Soil, Climate and Water (ARC-ISCW), South Africa
[3]Geography Environmental Management Energy Studies, University of Johannesburg, South Africa

DOI: https://dx.doi.org/10.4314/sajg.v13i2.7

Abstract

Mapping smallholder maize farms in complex and uneven rural terrain is a major barrier to accurately documenting the spatial representation of the farming units. Remote sensing technologies rely on various satellite products for differentiating maize cropland cover from other land cover types. The potential for multi-temporal Sentinel-1 synthetic aperture radar (SAR), Sentinel-2, digital elevation model (DEM) and precipitation data obtained from Climate Hazards Group InfraRed Precipitation with Station data (CHIRPS) version 2.0 was investigated for mapping maize crop distributions during the growing seasons, 2015–2021, in the Sekhukhune municipal area of Limpopo, a province in South Africa. Sentinel-1 variables, including monthly VH, VV, VV+VH (V = vertical, H = horizontal) polarization band data and data issuing from the principal component analysis of VH polarization were integrated with Sentinel-2-derived normalized difference vegetation index (NDVI), DEM terrain, and precipitation data. The random forest (RF) algorithm was applied to distinguish maize crops from four other land cover types, including bare soil, natural vegetation, built-up area, and water. The findings indicated that the models that used only Sentinel-1 data as input data had overall accuracies below 71%. The best performing models producing overall accuracies above 83% for 2015–2021 were those where Sentinel-1 (VV+VH) data were integrated with all the ancillary data. Overall, the McNemar test indicated enhanced performance for models where all other ancillary input data had been incorporated. The results of our study show considerable temporal variation in maize area estimates, with 59 240.84 ha in the 2018/2019 growing season compared to 18 462.51 ha in the 2020/2021 growing season. The spatial information gathered through these models proved to be valuable and is essential for addressing food security, one of the objectives of the Sustainable Development Goals.

Keywords: *remote sensing; synthetic aperture radar; optical satellite; normalized difference vegetation index; random forest; crop classification*

1. Introduction

Smallholder agriculture plays a pivotal role in ensuring global food security, especially in developing countries in Africa, South America and Asia (Bosc et al., 2013). In sub-Saharan Africa, approximately 96% of the population are smallholder farmers and are responsible for 90% of crop production (Hazell et al., 2002). However, under the influence of global change and the growing demand for food, small-scale farmers are inevitably under severe pressure to produce high-yielding crops to ensure food security (International Fund for Agricultural Development, 2013). To combat the effects of climate change and food insecurity, the smallholder farming sector urgently needs to adopt sustainable farming practices. Despite this need, insufficient spatial agroclimatic information has been gathered for planning and developing suitable management strategies (Shiferaw et al., 2011). The mapping of the long-term multi-temporal spatial distributions of smallholder farms is essential for a better understanding of their spatial distribution trends over time (Stuch et al., 2021).

Annual changes in smallholder crop outputs result from various factors, including fluctuations in local market prices and outdated crop production methods (Kebede, 2020). The prevailing climatic conditions and the availability of fertilizers and government subsidies are further factors leading to variations in smallholder crop outputs (Zerssa et al., 2021). Governments and decision-makers face challenges in their monitoring and provision of support to smallholder farming systems (Andrade et al., 2021; Mudhara and Senzanje, 2020). These systems are usually fragmented and located in remote and inaccessible areas, thus making them expensive to survey under traditional methods (Kerner et al., 2020b). Furthermore, methods of classifying and measuring the extent of smallholder cropland extent are still not sufficiently accurate (Aduvukha et al., 2021; Dlamini et al., 2023; Ren et al., 2022).

Information on the extent of smallholders in heterogeneous landscapes is needed to determine the actual area producing specific crops. In Limpopo, 49% of households contribute to agricultural activities, and six percent (6%) of these households are located in the Sekhukhune District Municipality (Sekhukhune District) (Statistics South Africa, 2011). Therefore, the mapping of smallholder farms is necessary to ensure food security, both in determining actual maize production and by informing yield forecast models (Jin et al., 2019). This spatial information is essential when planning farmer support, resource allocation and policy planning by governments in managing issues related to food security and climate change for smallholder farmers. To ensure food security for their households, most smallholder farmers grow maize for subsistence purposes (Masekoameng and Molotja, 2016). Because they are focused on domestic consumption, their crops are not available on the formal and informal markets. Research to develop robust and efficient techniques for mapping and monitoring smallholder farming landscapes is therefore necessary. Additionally, it is important to develop frameworks to represent the geographical distribution, cultivated area and temporal dynamics of smallholder farms (Vogels et al., 2019). These techniques will enhance our understanding of smallholder systems and will contribute to the attainment of the Sustainable Development Goals (SDGs), thus ensuring, amongst others, global food security.

Traditional crop mapping techniques were primarily based on *in situ* data collection methods such as field surveys and manual ground collection methods. These methods are labour intensive and expensive, whereas remote sensing techniques capture data at larger spatial extents (Mahlayeye et al., 2022). Certain remote sensing techniques for specifically assessing maize production in heterogeneous landscapes are promising (Chivasa et al., 2017). In fact, the advancement of remote sensing technologies has accelerated over the last few years with the development of big data retrieval and analysis platforms such as Google Earth Engine (GEE).

In the context of geoscience, the term, big data, generally refers to data collected from geospatial sources, remote sensing, ground surveying, geo-located sensors and mobile mapping (Tamiminia et al., 2020) that can then be further used for the processing, fusion, and mining of data (Li et al., 2021). Advanced image processing techniques represent a major benefit of GEE in that they provide valuable insights to support smallholder crop analysis, management, and decision-making. The benefit of processing larger datasets within the GEE platform is that image processing task loads are significantly simplified in that they also combine various datasets (Kibret et al., 2020). High-performance cloud computing in GEE allows for the rapid processing of large spatial datasets in crop studies, which would otherwise be significantly more time-consuming (Amani et al., 2020).

Selecting a classification method is essential for high-accuracy crop mapping. Machine learning algorithms are commonly used in crop classification, with the random forest (RF) classifier being widely used because of its success in reducing model overfitting and in promoting high-accuracy crop mapping (Mpakairi et al., 2023; Trivedi et al., 2023; Abubakar et al., 2023). Furthermore, various studies have shown that RF can be used to enhance model performance for mapping smallholder farms (Abubakar et al., 2020; Orynbaikyzy et al., 2022). For example, the study by Ren et al. (2022) mapped smallholder crop types in heterogenous landscapes in Africa and found RF to produce high classification accuracies (overall accuracy > 85%).

Synthetic aperture radar (SAR) is a radar remote sensing technique typically operating in the microwave region (bands X, C and L) of the electromagnetic spectrum. Unlike optical satellite sensors, SAR uses microwaves that penetrate clouds and other atmospheric interferences (Luo et al., 2021). One of the key advantages of SAR in crop monitoring is its ability to measure differences in backscattering coefficients, which vary according to the different crop growth stages (Arslan et al., 2022). This comes from SAR's ability to penetrate through the crop canopy, making it sensitive to changes in crop structure (Nasirzadehdizaji et al., 2021). The SAR is particularly sensitive to changes in crop structure during the early stages of growth when the maize plant is still relatively short and inclined to undergo more changes in height (Nasirzadehdizaji et al., 2019). Advancements have been made in the mapping of smallholder maize using multi-temporal SAR data rather than a single-date classification (Li et al., 2019). Relying on multi-temporal data is advantageous for achieving higher classification accuracy and also for the identification of the optimal temporal window for crop analysis (Vuolo et al., 2018). Furthermore, multi-temporal data obtained from optical and SAR data provide a better understanding of the phenological characteristics of the maize growth stages, thus

improving the efficiency of crop classifications (Shuai et al., 2019). As opposed to the use of individual spectral bands, such as red, green, blue and near-infrared, in the classification of smallholder maize farms, the incorporation of the normalized difference vegetation index (NDVI) has also been shown to improve the accuracy of readings taken throughout the growing season (Wen et al., 2022).

Brewer et al. (2022) reported that the near-infrared (NIR) region is essential for model estimations during the mid-vegetational growth stages. These authors found that spectral reflectance and NDVI are useful for indicating crop growth and vigour on smallholder maize farms in Malawi. Meanwhile, in Kenya, Ni et al. (2022) identified the importance of vegetation indices, specifically NDVI, for maize classifications during the rainfall season. This finding is particularly relevant to our study, as we conducted maize classification over a number of years and in the context of varying amounts of rainfall.

Very often, because of differences in crop patterns, planting times, temperature, precipitation, soil and terrain, the environment of smallholder crops is not uniform across the landscape. The integration of ancillary datasets with SAR data is necessary to address these differences and to better enhance the process of distinguishing between the various land cover types in these fragmented and heterogeneous terrains. The digital elevation model (DEM) is an essential dataset for correcting topographic information such as slope and elevation (Useya and Chen, 2019; Azzari et al., 2021). Slope can cause changes in the angle of incidence of Sentinel-1 data, resulting in variability in the Sentinel-1 backscattering properties. This, in turn, affects the accuracy of distinguishing maize crops from low vegetational cover in hilly, uneven or mountainous terrains (Li et al., 2015).

Rainfall is an important indicator of crop productivity because low rainfall negatively impacts maize growth. Detecting rainfall amounts from various climate models provides valuable insights into the success of the models in crop yield estimations. The Climate Hazards Group InfraRed Precipitation with Station (CHIRPS) was used in predicting precipitation levels affecting maize crops (Omondi et al., 2021). In a separate study, Masiza et al. (2022b), the CHIRPS model was reported to be highly correlated with *in situ* rainfall data for the South African smallholder maize cropland.

While no specific statistics were recently available for the Limpopo smallholder maize sector, the Crop Estimates Committee of South Africa reported that for the 2021 season, non-commercial maize amounted to 3.77% of the total tonnage of maize produced in South Africa. Estimates show that only 1.36% (37 500 ha) of this was from Limpopo province. However, this amount could be significantly higher since a a substantial percentage of smallholder data goes unrecorded. There is, therefore, a need to explore the utility of remote sensing in mapping smallholder farms to support accurate accounting of the spatial distribution of crops on such farms.

The purpose of this study was to identify the most suitable model for mapping smallholder maize crop distribution using Sentinel-1 imagery and ancillary spatial data sources. The specific objectives of the study were:

i) To determine whether various combinations of multi-temporal Sentinel-1 imagery, terrain, climate and/or Sentinel-2 NDVI spatial products improve the regional maize classification system;

ii) To identify the most suitable model for mapping smallholder maize crop distribution using Sentinel-1 imagery and ancillary spatial data sources;

iii) To formulate policy recommendations based on smallholder mapping and maize area estimates.

2. Materials and Methods

2.1. Study Site

The study was conducted in the Sekhukhune District in the south-eastern portion of Limpopo, a province in South Africa (Figure 1). The study area covers approximately 13 527.72 km^2 and encompasses a region of mostly rural smallholder farming villages, with Groblersdal being the largest town in the municipal area. The region is classified into three main ecoregions, namely the Bushveld Basin, the Eastern Bankenveld and the Northern Escarpment Mountains. The topography of these regions varies across the municipal area, which includes plains, hills and moderate to high mountains (with altitudes ranging between 500 and 23 00 m above mean sea level. Each ecoregion is characterized by unique climatic conditions in terms of temperature and rainfall. Higher rainfall averages are characteristic of the Eastern Bankenveld and Northern Escarpment Mountains where the mean annual precipitation ranges from 300 mm to 1 000 mm and 500 mm to 1 000 mm, respectively (Kleynhans et al., 2005). The Bushveld Basin ecoregions indicates a lower annual precipitation with a range of 400 mm to 600 mm. The mean annual temperature for all three regions ranges between 14 °C and 22 °C (Kleynhans et al., 2005).

The Sekhukhune municipal area falls into a semi-arid region that has an inconsistent rainfall pattern and is lacking in investment in smallholder agriculture. According to Mpandeli et al. (2015), smallholder farmers in the greater Sekhukhune District are vulnerable to extreme climatic variability as a consequence of droughts that impact the production of crops. Smallholder farmers in the study area lack irrigation systems and rely mainly on rainfall. The limited availability of water resulting from the variable climate means that croplands are being abandoned by farmers (Nzuza et al., 2022; Drimie et al., 2009). The terrain throughout the municipal area varies, with mountainous terrain in the north eastern areas where human activities such as crop cultivation are less likely to occur (Nzuza et al., 2022). Because there is a similarity between the semi-arid environment of the Sekhukhune District and other smallholder farming areas in South Africa, the district is a key area of interest in our study on smallholder maize farmers.

By delineating an area of interest within the smallholder boundary, as depicted in Figure 1, the researchers decided to exclude any agricultural operations conducted in the backyards of residents. Consequently, only land that had been demarcated as smallholder farmland was considered for

investigation. The geology in the municipal area predominantly includes a portion of the Rustenburg Granite Suite and the Lebowa Granite Suite, both constituting the Bushveld Complex (Geological Survey, 1986). The soil type in this region has a low average clay content, ranging from 15% to 19%, and pH levels that are ideal for crop growth (Mokgolo and Mzezewa, 2022). Concerns regarding food insecurity in the municipal area are on the rise. According to Mbhenyane et al. (2020), their study revealed that 77.2% of households in rural communities are experiencing food shortages. Furthermore, 78.9% of these households do not have access to vegetable gardens or fields for crop growth.

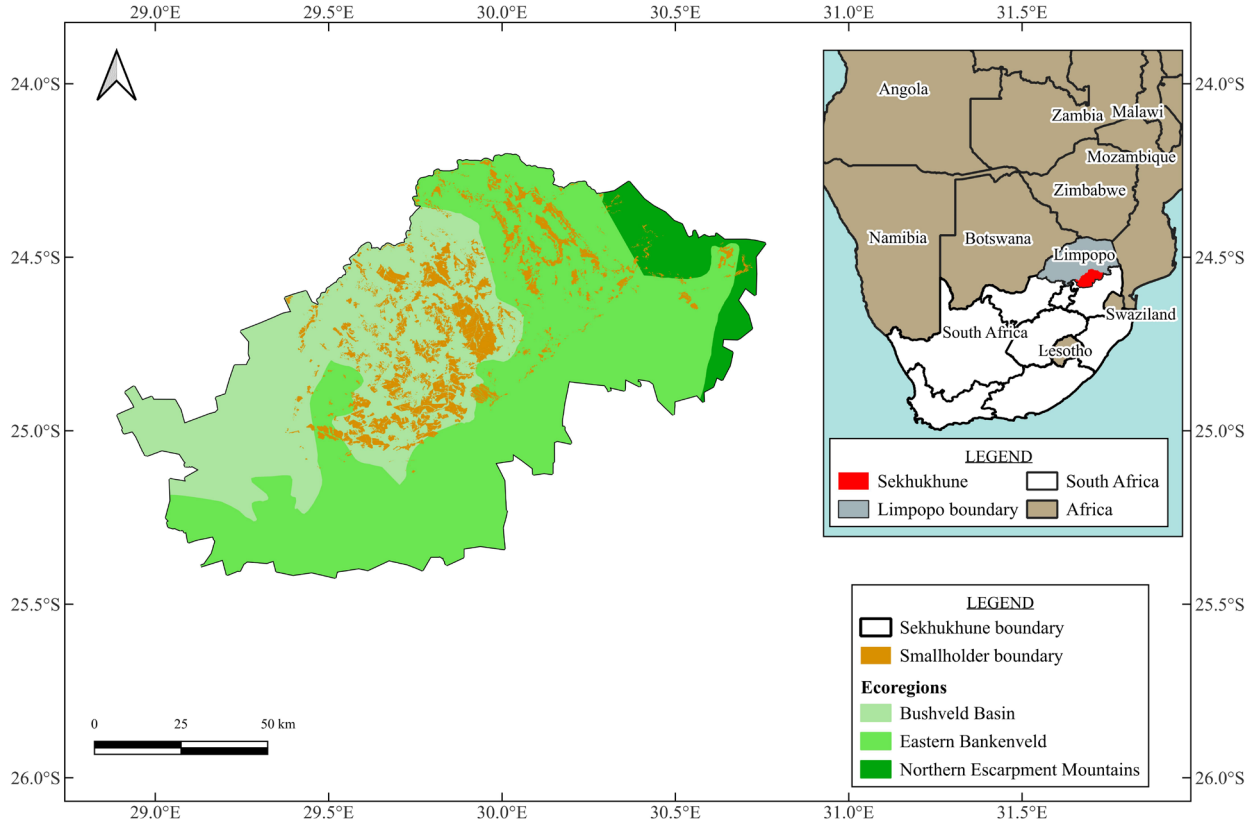

Figure 1. Map of Sekhukhune in Limpopo province, South Africa, showing smallholder boundaries and three ecoregions at a scale of 1:1 000 000, as classified by Kleynhans et al. (2005).

2.2. Reference Data Collection

The field campaign for collecting reference data extended over the period, 25 January to 8 February 2021. It involved the identification of smallholder farms and other land uses and incorporated data collection as an important process in the quest to identify training and validation data for the 2020/2021 growing season. The Garmin Montana 680t touchscreen handheld global positioning system, manufactured by Garmin (Olathe, Kansas, USA), with an accuracy of ≤ 3 m served to establish the coordinates for the various land use samples. The process involved digitising each growing season from 2015 to 2021 by using the marker tool in GEE to select the reference

points. Various regions of interest were assigned to the different land use classes, which then served as the reference data for training and validation purposes. For each year, the final dataset consisted of 100 data points for each of the five land use classes. These include maize, bare soil, natural vegetation, built-up area, and water.

The maize class was the main crop of focus because other non-maize classes, such as sugar beans, watermelons and pumpkins found growing among the maize plants were beneath the maize canopy. The spectral signatures of various low-growing crop classes are significantly obscured when they grow under the canopy of the maize crop (Jin et al., 2019). Also noteworthy is that in seeking to establish the spectral differences between maize and the afore-mentioned non-maize crops in this current study, the 10-metre resolution satellite imagery performed poorly. This difficulty was primarily due to the increased density of the maize canopy in tandem with the stage of the growing season. Distinguishing maize from intercropped species such as beans and cassava is a complex process because the overlapping spectral signatures are dependent on the crop patterns and the density of the maize crop (Hegarty-Craver et al., 2020).

Because the 2020/2021 season was the study period selected for collecting the field maize data, it was necessary to develop an approach to gather data for the years 2015/2016–2019/2020. The visual interpretation approach, which was subsequently adopted relied on maize referenced data from the 2020/2021 growing season and the period, October to May, was used to derive mean PCA images from the VH polarization band. The maize fields in these images were distinguished through their bright colours – either light green or yellow. This approach facilitated the identification of reference samples for each season from 2015 to 2020 in instances where the field survey data were not available.

Data for the other land use classes were collected from Sentinel-2 and Google satellite imagery through visual interpretation. This involved identifying and classifying various land use types such as waterbodies, soil, natural vegetation, and built-up areas. Field data and visual interpretation samples were needed to validate the selection of each class, which offered a crucial step in ensuring that the dataset accurately represented the real-world conditions of the study area. Overall, this approach helped to increase the researchers' confidence in the remote sensing data and ensured its accuracy and reliability in the context of the study.

2.3. Sentinel-1 Dataset

The European Space Agency developed the Copernicus Sentinel-1 dual polar-orbiting radar satellite constellation (Filipponi, 2019). The radar system is a C-band dual-polarization type, consisting of HH-HV or VV-VH modes (V = vertical, H = horizontal). Data are freely accessible on the Sentinel data hub (https://scihub.copernicus.eu/dhus) or GEE (https://code.earthengine.google.com/). The Sentinel-1 collection is available in GEE as Level 1 Ground Range Detected products that are detected and multi-looked to the 10×10 m grid size using the earth ellipsoid model (European Space Agency, 2024a). The collection has been pre-processed using the Sentinel-1 toolbox for users to access calibrated and orthorectified images (European Space Agency, 2024b).

The researchers used scenes which covered the entire Sekhukhune District. Each available image in the interferometric wide swath mode was selected per maize growing season from October to May, 2015 to 2021. For each year, monthly averages were established for both the VV and VH polarization bands; these monthly bands were then combined into one seasonal composite.

The backscattering coefficient temporal time series plots for the maize and other land cover types were created from the in-field collection of land cover data using Sentinel-1 data for the period, October 2020 to May 2021 (Figure 2). These included the plots for both the VV and VH polarization channels. According to Figure 2, the VH polarization channel is more sensitive to the phenological characteristics of the crop than those of the VV channel. This was evident, when the researchers compared the trend of the VH channel for maize and found that the VH backscattering coefficients were lower in the initial stages of maize growth. The backscattering coefficients were mostly below -20 dB between October 2020 and January 2021. For this same period, the VV channel showed backscattering coefficients that were limited to the -10 dB and -15 dB coefficients.

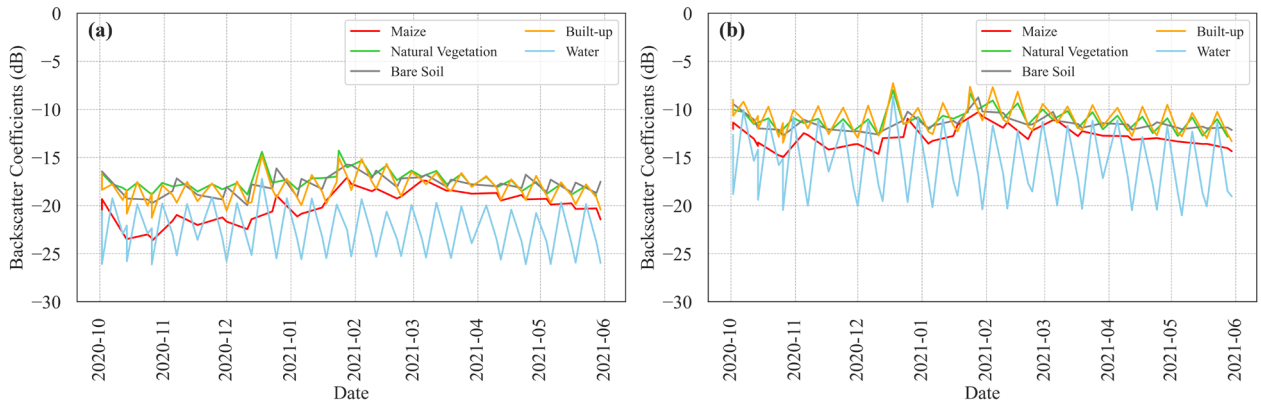

Figure 2. Temporal time series plots of the backscattering coefficient for different land cover classes at the (a) VH and (b) VV channels from October 2020 to May 2021.

The VH monthly composite was also further processed through principal component analysis (PCA), an image reduction technique described in Mashaba-Munghemezulu et al. (2021b). The current study used PCA to reduce the dimensionality of the monthly Sentinel-1 data (Jolliffe, 2002). To achieve more comprehensive and improved models in the context of our study, additional satellite data were therefore incorporated into the models. These included the digital elevation model (DEM), the Climate Hazards Group InfraRed Precipitation with Station (CHIRPS) rainfall data, and the Sentinel-2 derived normalized difference vegetation index (NDVI).

2.4. Ancillary Data

There are various spatial and climate datasets available on the Google Earth Engine (GEE) platform, including Sentinel-1, Sentinel-2, Landsat Legacy, Moderate Resolution Imaging Spectroradiometer (MODIS) Terra MOD09A1 Version 6.1, the fifth generation of European Reanalysis (ERA5-Land) and Tropical Rainfall Measuring Mission (TRMM) 34B2. They can easily be incorporated into the classification models by using GEE, since, by default, the last-mentioned reprojects products by using the nearest neighbour resampling analysis.

Table 1 lists the sensor characteristics for the monthly ancillary data selected for this study; these data included DEM, NDVI and precipitation data. The version 3 DEM with 30 m resolution was acquired using Shuttle Radar Topography Mission (SRTM) (Farr et al., 2007) to calculate slope and elevation. These two important variables should be included in the mapping of smallholder maize fields because farmers plant crops even on relatively steep slopes. The monthly NDVIs were calculated from the red and near-infrared bands of the Sentinel-2 Multispectral Instrument (MSI). Also, previous research found the NDVI to be an important variable in mapping maize crops (Liepa et al., 2024; Kerner et al., 2020a). Sentinel-2 Level-2A imagery was available in GEE for the period, 2018/10 to 2021/05. Since Level 2A Sentinel-2 data for 2015/10 to 2018/05 were not available, Sentinel-2 Level-C1 imagery were downloaded from the Copernicus browser (https://dataspace.copernicus.eu/browser/), using the Sen2Cor module in Python to manually pre-process the images for atmospheric correction (Louis et al., 2019; Main-Knorn et al., 2017). After cloud masking, a mean NDVI image per growing season was generated for inclusion in the models that were loaded to GEE. The precipitation band from the CHIRPS Pentad: Climate Hazards Group InfraRed Precipitation climate version 2.0 (Funk et al., 2015) data, with a 5 000 m resolution, for the entire season was incorporated into the models. Recently, as opposed to the Tropical Applications of Meteorology that use satellite and ground-based data (TAMSAT), CHIRPS has been identified as a good estimator of rainfall as it has been found to be highly correlated with *in situ* precipitation data in the smallholder landscape (Masiza et al., 2022a; Masiza et al., 2022b). This product is necessary since it identifies critical periods of high rainfall conditions that would contribute significantly to smallholder maize growth. These datasets were all incorporated into our models to determine whether they would contribute to the mapping of smallholder maize crops on a regional scale.

Table 1. Summary of data used in the study

	Sentinel-1	**Sentinel-2 NDVI**	**CHIRPS**	**DEM**
	Sensor properties			
Central Wavelengths	5.405 GHz	443, 490, 560, 665, 705, 740, 783, 842, 865, 945, 1375, 1610, 2190 nm		
Band Width	0-100 MHz	20-180 nm		
Spatial Resolution (m)	10	10, 20, 60	5000	30
Temporal Resolution (days)	12	5	1	N/A
Image acquisition dates	**Number of images**			
2020/10/01-2021/05/25	195	321	46	1
2019/10/01-2020/05/25	197	363	46	1
2018/10/01-2019/05/25	177	254	46	1
2017/10/01-2018/05/25	199	208	46	1
2016/10/01-2017/05/25	93	182	46	1

Table 1 presents the count of images per dataset and outlines the timeframe during which imagery was collected across the six growing seasons. The selection of image acquisition dates was specifically designated for the period, October to May. The monthly image collection process spanned

the entire growing season; thus it was possible to address the challenges faced by smallholder farmers who might not have precise planting dates because of their dependence on rainfall, government subsidies and the availability of funds for purchasing seeds or equipment. As such, it is inherently difficult for them to establish a precise cropping calendar.

2.5. Image Classification

A land cover classification for the study was carried out by using the supervised random forest (RF) machine-learning algorithm (Breiman, 2001). This method has been shown to perform well in the classification of smallholder farms and involves the differentiation of maize and other land cover types (Abubakar et al., 2020). The RF classifier can handle high data dimensionality and is not subject to overfitting (Breiman, 2001). Since bootstrapping allows for the building of decision trees for the creation of a forest, it was the preferred technique that was used to achieve the relevant algorithm.

The hyperparameters that were subsequently selected required the selection of a specific number of decision trees and of variables to split, both amounting to the square root of the number of variables. The ground truth dataset, which was randomly split into 80% training and 20% validation data, used the training data as the input data for the RF classification. The classification was then incorporated into the GEE, with the output images thus obtained at a spatial resolution of 10 m.

2.6. Methodology Overview and Model Designs

Figure 3 shows an overview of the processing involved in mapping the smallholder maize distribution in Sekhukhune District. The six main steps thus involved were as follows: First, data collection included the compilation of monthly Sentinel-1 imagery, Sentinel-2, DEM, CHIRPS, and the incorporation of ground truth data into GEE for training and the validation of the models. Second, image pre-processing consisted of the extraction of monthly Sentinel-1 VH and VV images, the generation of NDVI images, the transformation of DEM data into slope and elevation data and the extraction of monthly precipitation figures from the CHIRPS dataset. Third, 24 model combinations were created by integrating Sentinel-1 data with other ancillary datasets. The fourth step consisted of splitting the ground truth data into training and testing data, with a split ratio of 80% to 20%. Subsequently, the RF algorithm was employed to predict the classes of the new predicted maize and land cover data. At this stage, the testing subset served to evaluate the model's performance for validation. The fifth stage involved the post-classification processing of the data and model evaluation. These processes involved the use of the 'gdal_sieve.py' algorithm in QGIS to remove the small pixels and replace them with the nearest neighbour pixel value. Additionally, smallholder boundaries, as depicted in Figure 1, were clipped to isolate the region of interest using the 'clip-raster-by-mask-extent' algorithm in QGIS. This process served to delineate the boundaries of smallholder maize farms in the former homelands in Sekhukhune District. An accuracy assessment was conducted and statistical analyses were employed to evaluate the performance of the 24 models.

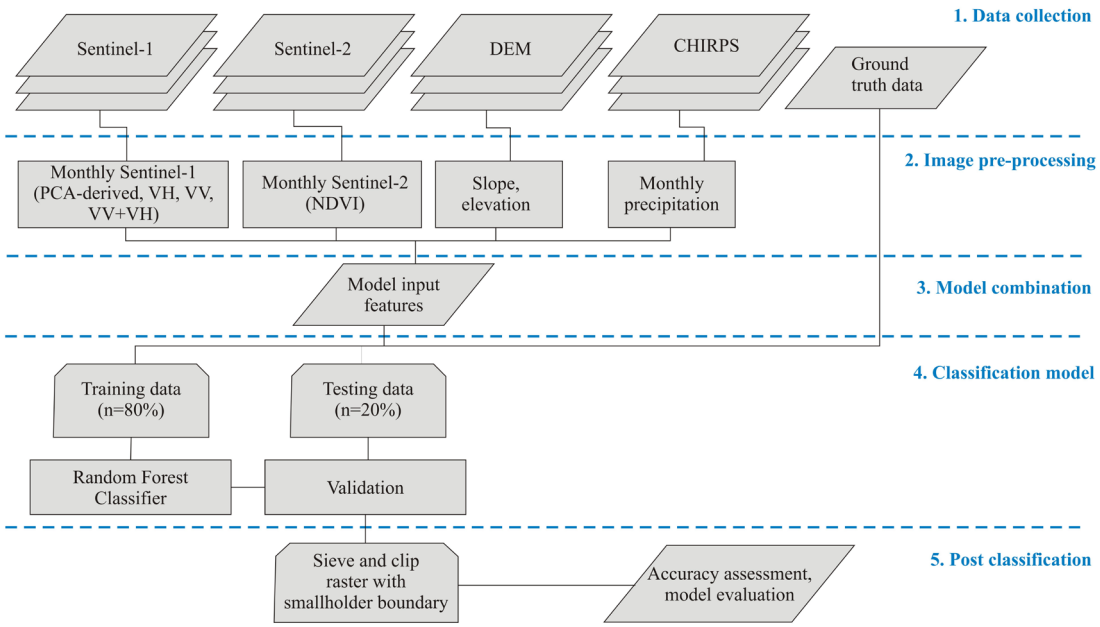

Figure 3. The schema of methodology for this research.

Table 2. The 24 variations of model combinations of Sentinel-1 data integrated with ancillary datasets.

	Model Input Features
Model 1	Sentinel-1 PCA_VH only
Model 2	Sentinel-1 PCA_VH, slope, elevation
Model 3	Sentinel-1 PCA_VH, slope, elevation, rainfall
Model 4	Sentinel-1 PCA_VH, Sentinel-2-NDVI
Model 5	Sentinel-1 PCA_VH, slope, elevation, Sentinel-2-NDVI
Model 6	Sentinel-1 PCA_VH, slope, elevation, Sentinel-2-NDVI, rainfall
Model 7	Sentinel-1 VH_monthly only
Model 8	Sentinel-1 VH_monthly, slope, elevation
Model 9	Sentinel-1 VH_monthly, slope, elevation, rainfall
Model 10	Sentinel-1 VH_monthly, Sentinel-2-NDVI
Model 11	Sentinel-1 VH_monthly, slope, elevation, Sentinel-2-NDVI
Model 12	Sentinel-1 VH_monthly, slope, elevation, Sentinel-2-NDVI, rainfall
Model 13	Sentinel-1 VV_monthly only
Model 14	Sentinel-1 VV_monthly, slope, elevation
Model 15	Sentinel-1 VV_monthly, slope, elevation, rainfall
Model 16	Sentinel-1 VV_monthly, Sentinel-2-NDVI
Model 17	Sentinel-1 VV_monthly, slope, elevation, Sentinel-2-NDVI
Model 18	Sentinel-1 VV_monthly, slope, elevation, Sentinel-2-NDVI, rainfall
Model 19	Sentinel-1 VV+VH_monthly only
Model 20	Sentinel-1 VV+VH_monthly, slope, elevation
Model 21	Sentinel-1 VV+VH_monthly, slope, elevation, rainfall
Model 22	Sentinel-1 VV+VH_monthly, Sentinel-2-NDVI
Model 23	Sentinel-1 VV+VH_monthly, slope, elevation, Sentinel-2-NDVI
Model 24	Sentinel-1 VV+VH_monthly, slope, elevation, Sentinel-2-NDVI, rainfall

The long-term availability of satellite datasets in GEE has made the platform a powerful classification tool. Owing to its ease of integration with the GEE platform and its ability to process substantial amounts of data, the RF classifier has proved its worth in classifying smallholder crops. The integration of Sentinel-1 imagery with the various ancillary datasets (e.g. Sentinel-2) is a technique known as data combination. This involves the combination of two or more datasets as input features for modelling. This method enhances the accuracy of the results by merging complementary information from various data sources. For example, Masiza et al. (2020) illustrated that by combining Sentinel-1 and Sentinel-2 data, greater accuracy could be achieved in the mapping of smallholder maize than by using only optical data in a stacked model approach. Table 2 presents all the model variations created in this study.

2.7. Accuracy Assessment, Area Estimated Accuracy and Variables

An accuracy assessment enabled the researchers to evaluate the classification results of this study. Validation data were selected randomly from the relevant ground truth dataset to estimate the accuracy of the RF classification. After the initial classification, the confusion matrix was extracted from the classification results in GEE and the overall accuracy (OA), producer's accuracy (PA), user's accuracy (UA), and kappa statistics (K), all of which were described by Congalton and Green (2019), and calculated as follows:

$$OA = \frac{1}{N}\sum_{i=1}^{c} n_{ii}, \quad (1)$$

$$PA = \frac{n_{ii}}{n_{icol}}, \quad (2)$$

$$UA = \frac{n_{ii}}{n_{irow}}, \quad (3)$$

$$K = \frac{1}{N}\sum_{i=1}^{c} n_{ii} - \sum_{i=1}^{c} \frac{n_{icol}n_{irow}}{N^2} - \sum_{i=1}^{c} n_{icol}n_{irow}, \quad (4)$$

Where

n_{ii} is the number of correctly classified pixels in a class; N is the total number of pixels within the confusion matrix; c is the number of classes; n_{irow} is the total number of sample pixels in the row (the predicted class); and n_{icol} is the total number of sample pixels in the column (the reference class).

The success of the overall classification is displayed in the OA, with values closest to 1 indicating a good classification. The classifiers' results were used to extract the importance of each variable in the mapping of smallholder maize. This metric, showing the importance of the respective variables, highlights the contribution of each variable to the model-building process. The kappa coefficient of agreement is an indication of the concurrence between the classification results and the reference data. Kappa values higher than 0.8 show a strong concurrence between these variables, whereas values between 0.4 and 0.8 indicate a moderate concurrence, and values below 0.4 reflect a poor concurrence.

Based on the methodology described by Olofsson et al. (2013), the estimated mapped areas and confidence intervals for the unbiased area were then calculated. The areas (in hectares) were corrected at 95% confidence intervals and the margins of error were determined. By calculating the error-adjusted UAs, PAs and OA, this method improved the accuracy assessments.

2.8. Evaluating Statistical Significance of Model Performance

The study analysed various models to find the most suitable combination of data sources for mapping maize farming units. McNemar's approach was used to test the statistical significance of the best-performing model as opposed to the other models developed in this study. The Z-score was then calculated to compare the various models:

$$Z = \frac{|K_1 - K_2|}{\sqrt{var(K_1) - var(K_2)}} \quad (5)$$

Where

K1 indicates the kappa value for Model 1 and K2 is the kappa value for Model 2. The var (K1) and var (K2) expressions represent the variance of each of the respective models. The analyses that the models facilitated were to determine the significance of the respective associations between the respective variables based on the Z-score. $Z < 1.96$ indicates no significant difference in the accuracy between the two models, whereas $Z > 1.96$ shows a statistically significant difference in the accuracy between the two models. As such, it can be concluded that the second model differs significantly from the first (Montelpare and McPherson, 2000).

3. Results

3.1. Accuracy Assessment of Classified Images

Table 3 presents the error-adjusted overall accuracy (OA) for all 24 models covering the Sekhukhune District from 2015 to 2021. Derived from the random 20% validation data, these accuracies subsequently served to generate error-adjusted OA estimates for the area. For the models where only Sentinel-1 data were included (Model 1, 7, 13 and 19), and where principal component analysis (PCA) − incorporating only the VH polarization band (Model 1), VH_monthly data (Model 7), VV_monthly data (Model 13) and VV+VH_monthly data (Model 19) − was conducted, the error-adjusted OAs were found to be between 46.56% and 84.36% for the entire period, 2015 to 2021. These OA results are less than ideal for classification success, as a classification accuracy above 85% is considered favourable (Kpienbaareh et al. 2021).

Ancillary data were also incorporated into the models to improve classification accuracy. The PCA_VH and VH_monthly models with additional slope and elevation data, namely Models 2 and 8, showed improved error-adjusted OAs between 67.82% and 82.38%. However, the addition of slope and elevation data to the VV_monthly model (Model 14) and the VV+VH_monthly model (Model 20) presented accuracies between 75.37% and 90.72%.

Table 3. Accuracy assessment listed for the 24 respective classification models per maize growing season from 2015 to 2021.

Model no.	Model input features	2015/ 2016	2016/ 2017	2017/ 2018	2018/ 2019	2019/ 2020	2020/ 2021	Average
1	Sentinel-1 PCA_VH only	52.65	68.36	46.56	76.06	72.37	66.29	63.71
2	Sentinel-1 PCA_VH, slope, elevation	67.82	79.27	69.01	81.27	79.65	77.76	75.80
3	Sentinel-1 PCA_VH, slope, elevation, rainfall	73.22	84.13	74.51	83.34	73.85	77.99	77.84
4	Sentinel-1 PCA_VH, Sentinel-2-NDVI	70.55	78.29	73.79	85.17	84.46	92.06	80.72
5	Sentinel-1 PCA_VH, slope, elevation, Sentinel-2-NDVI	77.17	81.28	81.57	95.25	91.89	91.74	86.49
6	Sentinel-1 PCA_VH, slope, elevation, Sentinel-2-NDVI, rainfall	77.68	87.67	88.32	97.03	87.69	95.24	88.94
7	Sentinel-1 VH_monthly only	63.38	70.43	67.00	72.22	70.97	70.72	69.12
8	Sentinel-1 VH_monthly, slope, elevation	73.05	77.64	78.63	79.07	82.38	77.89	78.11
9	Sentinel-1 VH_monthly, slope, elevation, rainfall	76.12	82.27	79.70	82.52	83.58	77.62	80.30
10	Sentinel-1 VH_monthly, Sentinel-2-NDVI	77.10	79.23	77.19	85.69	87.81	89.20	82.71
11	Sentinel-1 VH_monthly, slope, elevation, Sentinel-2-NDVI	78.31	85.65	85.03	94.31	91.29	94.06	88.11
12	Sentinel-1 VH_monthly, slope, elevation, Sentinel-2-NDVI, rainfall	78.90	87.66	79.06	96.74	92.36	92.01	87.79
13	Sentinel-1 VV_monthly only	63.46	71.75	71.89	72.51	68.88	72.76	70.21
14	Sentinel-1 VV_monthly, slope, elevation	83.28	75.37	78.66	77.42	90.72	87.38	82.14
15	Sentinel-1 VV_monthly, slope, elevation, rainfall	86.21	83.45	83.07	78.71	86.82	91.70	84.99
16	Sentinel-1 VV_monthly, Sentinel-2-NDVI	79.23	81.22	74.14	86.32	84.96	91.81	82.95
17	Sentinel-1 VV_monthly, slope, elevation, Sentinel-2-NDVI	83.49	87.74	76.15	88.32	86.57	91.98	85.71
18	Sentinel-1 VV_monthly, slope, elevation, Sentinel-2-NDVI, rainfall	82.45	90.00	82.53	90.07	86.51	93.97	87.59
19	Sentinel-1 VV+VH_monthly only	62.22	77.26	66.21	84.36	78.76	74.22	73.84
20	Sentinel-1 VV+VH_monthly, slope, elevation	77.57	84.20	79.66	85.25	84.91	87.05	83.11
21	Sentinel-1 VV+VH_monthly, slope, elevation, rainfall	83.85	88.62	84.99	86.69	84.57	94.56	87.21
22	Sentinel-1 VV+VH_monthly, Sentinel-2-NDVI	74.04	88.47	72.03	89.26	90.34	90.41	84.09
23	Sentinel-1 VV+VH_monthly, slope, elevation, Sentinel-2-NDVI	81.73	87.72	79.41	93.48	91.18	94.56	88.02
24	Sentinel-1 VV+VH_monthly, slope, elevation, Sentinel-2-NDVI, rainfall	83.83	95.18	89.68	97.74	92.03	94.40	92.14

*****Accuracies above 85% in bold**

In the third model variation, slope, elevation and rainfall (CHIRPS) data were added to the Sentinel-1 data. The addition of the precipitation data produced only minor improvements in the error-adjusted OAs. In fact, the PCA_VH and VH_monthly models incorporating slope, elevation and rainfall data (Models 3 and 9) continued to produce accuracies below 85% compared to the VV_ and VV+VH_monthly models (Models 15 and 21) incorporating the same ancillary data and producing error-adjusted OAs between 78.71% and 94.56%. Initially, when Sentinel-2 NDVI data were added, the PCA_VH and VH_monthly models presented with error-adjusted OAs above 85%. The error-adjusted OAs for all four Sentinel-1 model types with the Sentinel-2 NDVI ancillary data ranged between 70.55% and 92.06%. The OAs improved (>76.15%) when slope and elevation data were introduced into the Sentinel-1 and Sentinel-2 NDVI models. The last model (Model 24) included all the ancillary datasets (slope, elevation, Sentinel-2 NDVI, and rainfall data). Overall, Models 6, 12, 18 and 24 produced results for all three Sentinel-1 variations, with error-adjusted OAs between 77.68% and 97.74%.

Over the maize crop growing seasons, extending from 2015 to 2021, Model 24 produced the highest average OA (92.14%). The land cover classification for this model produced PAs from 86.2% to 100% and UAs from 80% to 100% for the maize class. These are favourable, especially when one considers that the PAs and UAs for the maize class associated with this model were for six growing seasons. The second-highest OAs (88.94%) for the maize growing seasons, 2015 to 2021, were for Model 6. The classification for Model 6 produced PAs between 81.58% and 100% and UAs between 83.33% and 100% for the maize class. Based on these results, Models 6 and 24 were the best-performing models for producing high-accuracy maize classification results.

The maize class is the only crop type identified through this classification. Furthermore, the PAs and UAs for the other land cover classes for these two models were high. The lowest PAs for the maize growing seasons, 2015 to 2021 were in the built-up class; they ranged between 59.78% and 95.48% for Model 6 and between 66.14% and 100.00% for Model 24. The results for the 2015/2016 growing season consistently produced less accurate OAs, with only the Model 15 classification presenting an OA above 85%, while all the other models underperformed. The lower accuracy determined for the 2015/2016 maize growing season can be attributed to the lower accuracy of the sampling data since, as was the case with the data for 2020/2021, these statistics were collected via desktop and not in the field. Variability in smallholder planting dates can also be a factor influencing the lower performance accuracy of the classification models.

3.2. Statistical Analysis

Table 4 shows the results of McNemar's test which compared the statistical significance level of Model 6 (Sentinel-1 PCA_VH images with slope, elevation, Sentinel-2 NDVI and rainfall data) to those of the other 23 models for the maize growing seasons, 2015 to 2021. The Z-scores show that most of the models differed statistically from Model 6. The error-adjusted OA indicates that Models 6 and 24 were the two best-performing models, outperforming most of the models evaluated in this study. However, the Z-score shows that five of the other models, namely Models 5, 11, 12, 18 and

23, did not significantly differ statistically from Model 6 in terms of classification performance for at least five of the growing seasons.

Table 4. McNemar's test of the PCA Sentinel images, slope, elevation, NDVI and rainfall model compared to the other three models over the respective years from 2015 to 2021.

Model no.	Model input features	Model no. 6. Sentinel-1 PCA_VH, slope, elevation, Sentinel-2-NDVI, rainfall					
		2015/ 2016	2016/ 2017	2017/ 2018	2018/ 2019	2019/ 2020	2020/ 2021
1	Sentinel-1 PCA_VH only	6.04	5.47	5.78	6.01	7.10	4.82
2	Sentinel-1 PCA_VH, slope, elevation	3.47	2.58	4.75	3.85	4.30	3.20
3	Sentinel-1 PCA_VH, slope, elevation, rainfall	2.54	1.96	2.71	3.68	4.65	3.20
4	Sentinel-1 PCA_VH, Sentinel-2-NDVI	3.50	3.12	4.31	3.42	3.45	1.52
5	Sentinel-1 PCA_VH, slope, elevation, Sentinel-2-NDVI	1.31	2.30	1.65	1.09	1.09	1.52
7	Sentinel-1 VH_monthly only	5.66	5.25	5.55	6.08	6.42	5.20
8	Sentinel-1 VH_monthly, slope, elevation	3.16	3.32	3.73	5.00	4.33	4.44
9	Sentinel-1 VH_monthly, slope, elevation, rainfall	2.19	2.61	2.76	4.26	3.47	4.04
10	Sentinel-1 VH_monthly, Sentinel-2-NDVI	2.54	3.34	3.23	3.18	2.76	2.71
11	Sentinel-1 VH_monthly, slope, elevation, Sentinel-2-NDVI	1.79	1.61	1.67	1.91	1.55	1.06
12	Sentinel-1 VH_monthly, slope, elevation, Sentinel-2-NDVI, rainfall	1.27	0.12	3.19	1.55	0.11	1.52
13	Sentinel-1 VV_monthly only	6.13	5.78	4.99	6.03	6.35	5.00
14	Sentinel-1 VV_monthly, slope, elevation	2.05	4.79	3.45	4.96	2.54	3.53
15	Sentinel-1 VV_monthly, slope, elevation, Rain	2.36	3.82	3.50	4.81	3.25	2.99
16	Sentinel-1 VV_monthly, S2-NDVI	1.72	3.36	3.70	2.48	2.79	2.18
17	Sentinel-1 VV_monthly, slope, elevation, Sentinel-2-NDVI	2.05	2.62	2.95	2.21	1.57	2.19
18	Sentinel-1 VV_monthly, slope, elevation, Sentinel-2-NDVI, rainfall	1.74	1.62	1.22	1.91	1.92	1.52
19	Sentinel-1 VV+VH_monthly only	5.03	4.48	6.86	4.24	5.62	4.81
20	Sentinel-1 VV+VH_monthly, slope, elevation	1.24	3.90	4.24	3.65	3.91	3.20
21	Sentinel-1 VV+VH_monthly, slope, elevation, rainfall	2.06	2.39	3.10	3.87	3.70	2.49
22	Sentinel-1 VV+VH_monthly, S2-NDVI	2.87	2.01	4.38	2.49	2.24	2.18
23	Sentinel-1 VV+VH_monthly, slope, elevation, Sentinel-2-NDVI	1.69	1.11	2.95	1.09	1.93	1.52
24	Sentinel-1 VV+VH_monthly, slope, elevation, Sentinel-2-NDVI, rainfall	2.06	2.19	1.59	0.03	0.11	1.52

Threshold for statistical significance: $Z > 1.96$

These results indicate that these models produce consistently good classification results for mapping maize. The common variables that are present in all seven statistically similar models are the presence of the Sentinel-2 NDVI and rainfall data. This could indicate the advantage of incorporating these products into Sentinel-1 classifications of maize and of land cover.

3.3. Variable Importance

In the process of classifying land use for all six seasons, the contributions of individual variables in the respective models were computed. Figure 4 displays the variable importance scores (in %) for Models 6, 12, 18 and 24 in the classification of land use for the 2020 to 2021 growing season. Figure 4a shows the scores for Model 6, which used Sentinel-1 PCA_VH, as well as ancillary data, for slope, elevation, NDVI and rainfall. The results show that Sentinel-2 NDVI, Sentinel-1 VH PC1, Sentinel-1 VH PC2, Sentinel-1 VH PC3 and elevation were the most important variables in this model. The variable importance score for Model 12 (VH_monthly; Figure 4b) indicates that Sentinel-2 NDVI, Sentinel-1 VH-1, Sentinel-1 VH-7 and elevation data were the most important features for classification. This is opposed to Model 18 (VV_monthly; Figure 4c), with the most important variables being identified as Sentinel-2 NDVI and elevation data, followed by Sentinel-1 VV-6 and Sentinel-1 VV-3 data. The variable importance score for Model 24 (Figure 4d) indicates that Sentinel-2 NDVI, Sentinel-1 VV+VH-1 and elevation data were the three most important features of this model. These models are combinations of Sentinel-1 data with all the other ancillary datasets (slope, elevation, Sentinel-2 NDVI and rainfall data), with the most important variables identified being the Sentinel-2 NDVI, Sentinel-1 data and elevation data. When ranking the relative importance of the variables, rainfall data occupied mainly the fifth to seventh positions in the ranking hierarchy, with slope data featured in the eighth or lower position.

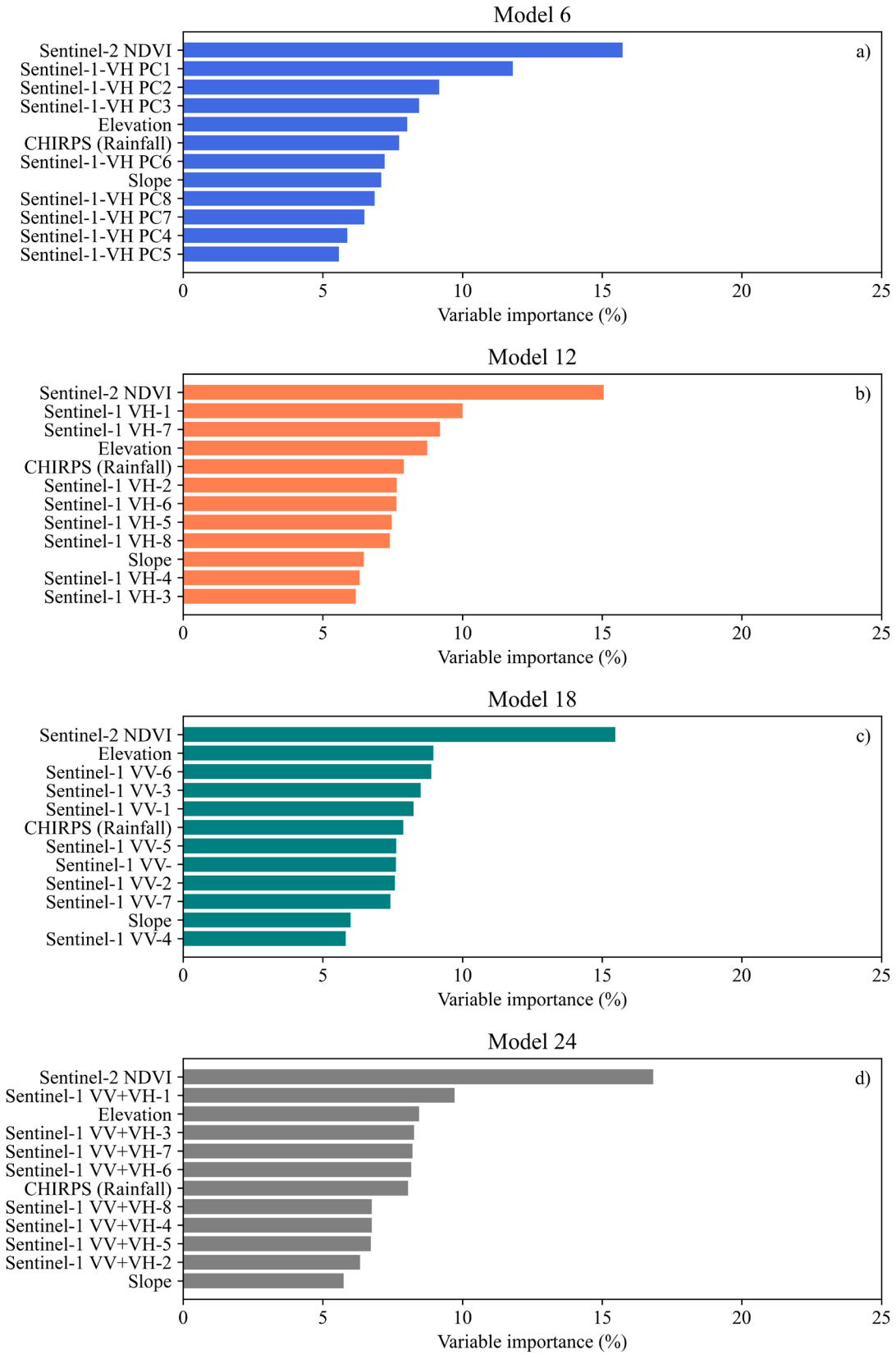

Figure 4. Variable importance graphs for Sentinel-1 channels and ancillary data in land use classification (2020-2021 growing season): they include a) PCA Sentinel-1 principal components (PC1 to PC8), monthly analysis of b) Sentinel-1 VH (VH-1 to VH-8), c) VV (VV-1 to VV-7), and d) combined VV+VH (VV+VH-1 to VV+VH-8), along with slope, elevation, NDVI, and rainfall data (October 2020 – May 2021).

3.4. Crop Classification

The crop classification maps derived from the Sentinel-1 and the ancillary data inputs (slope, elevation, CHIRPS rainfall and Sentinel-2 NDVI) are presented in Figure 5. These maps were generated from four of the 24 models for the Sekhukhune District study area in the 2020/2021 reference year. On visually comparing the results for the different combinations of the Sentinel-1 data inputs and the ancillary data inputs, misclassifications came too light. The greatest difference that was observed in the classification outputs was when Sentinel-2 NDVI data were combined with Sentinel-1 data. Yet another challenge faced – the most common of all – was the confusion that arose in differentiating between bare soil and natural vegetation cover, as shown in Figure 5b and Figure 5c, as opposed to Figure 5d. Furthermore, as shown in the classifications in Figure 5d, Figure 5e, Figure 5f and Figure 5g, Models 6, 12, 18 and 24 (that combined Sentinel-1 and Sentinel-2 NDVI data) resulted in the confusion of maize crop, bare soil, built-up and natural vegetation land use types. In addition, the classification results of Model 18 were less favourable owing to the presence of the 'salt-and-pepper' effect − observed in the form of small pixels scattered within the larger classified regions, as in the occurrence of maize pixels within the natural vegetation class.

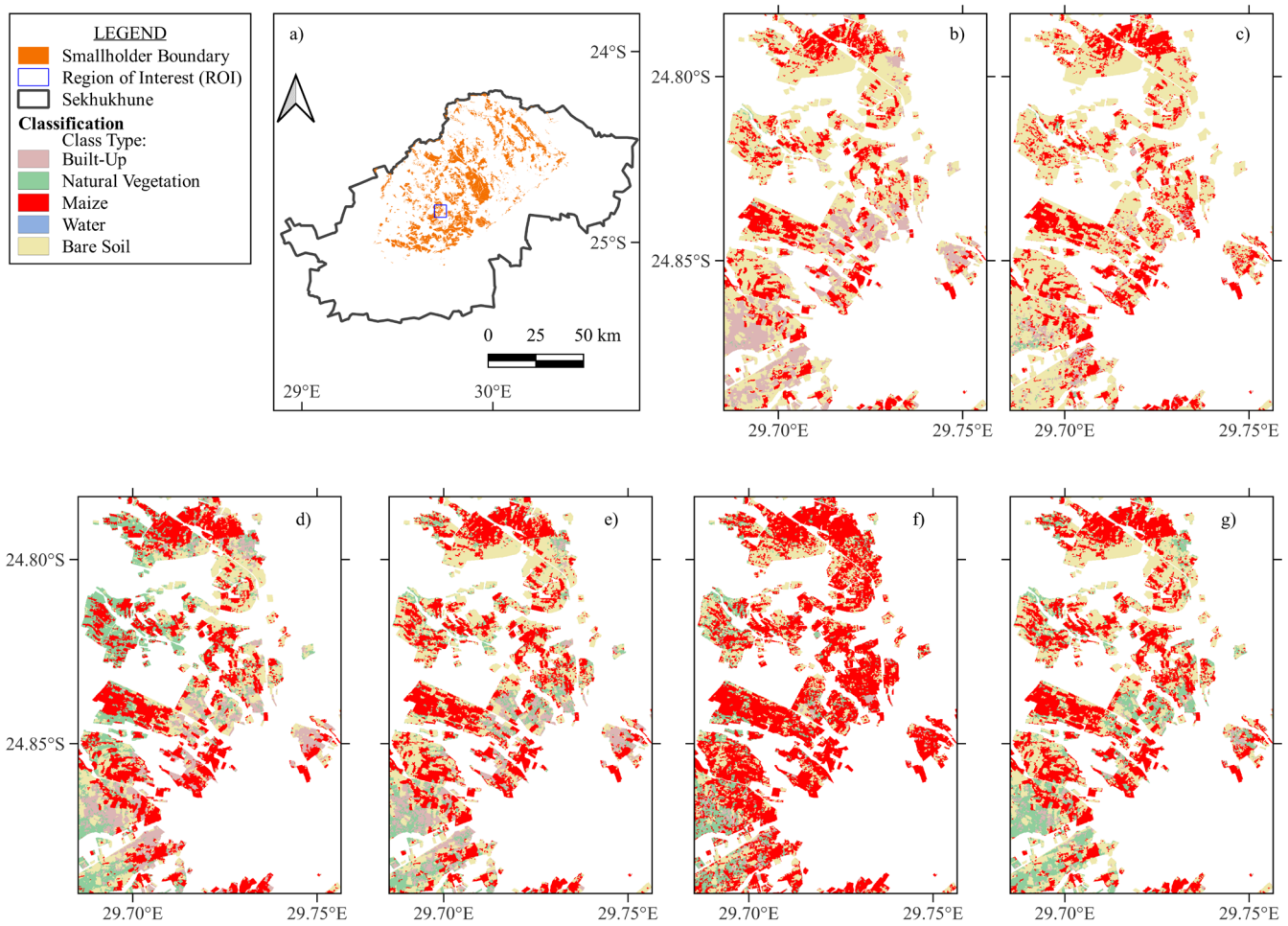

Figure 5. The map in (a) shows the entire Sekhukhune District Municipality with the smallholder farms layer and the region of interest that the (b) to (g) maps are zoomed into. The maps of maize and land cover classification, derived from monthly Sentinel-1 data and ancillary data (elevation, slope and rainfall), are shown in (b) Model 11 and (c) Model 17. The classification map with Sentinel-1 data and ancillary data (elevation, slope, Sentinel-2 NDVI and CHIRPS) is presented in (d) Model 6, (e) Model 12, (f) Model 18 and (g) Model 24.

3.5. Maize Area Estimates from 2015 to 2021

The maize area estimates determined for six maize-growing seasons were for the maize growing seasons, 2015 - 2021. The study focused on mapping smallholder maize cropland by calculating the unbiased proportional areas. The reference data were obtained from the South African National Land Cover (SANLC) 2020 dataset (Department of Forestry, 2020). The data retrieved indicate that 10 7871.88 ha of this study area were classified as subsistence/small-scale agriculture in 2020. The results mentioned in this section are for the best-performing experiment (Model 24). The area estimated for planted maize in Sekhukhune District varies considerably over time (Figure 6). The estimate for the area under maize in 2015/2016 amounted to 31 324 ha, but by the end of the 2016/2017 growing season, it had decreased to 18 462.51 ha. The largest area under maize (59 240.84 ha) was for the 2018/2019 growing season, but declined to 43 213.82 ha in 2019/2020. There was a continued decline in the area under maize cultivation within the study area for the 2020/2021 period, with it decreasing to 21 698.13 ha.

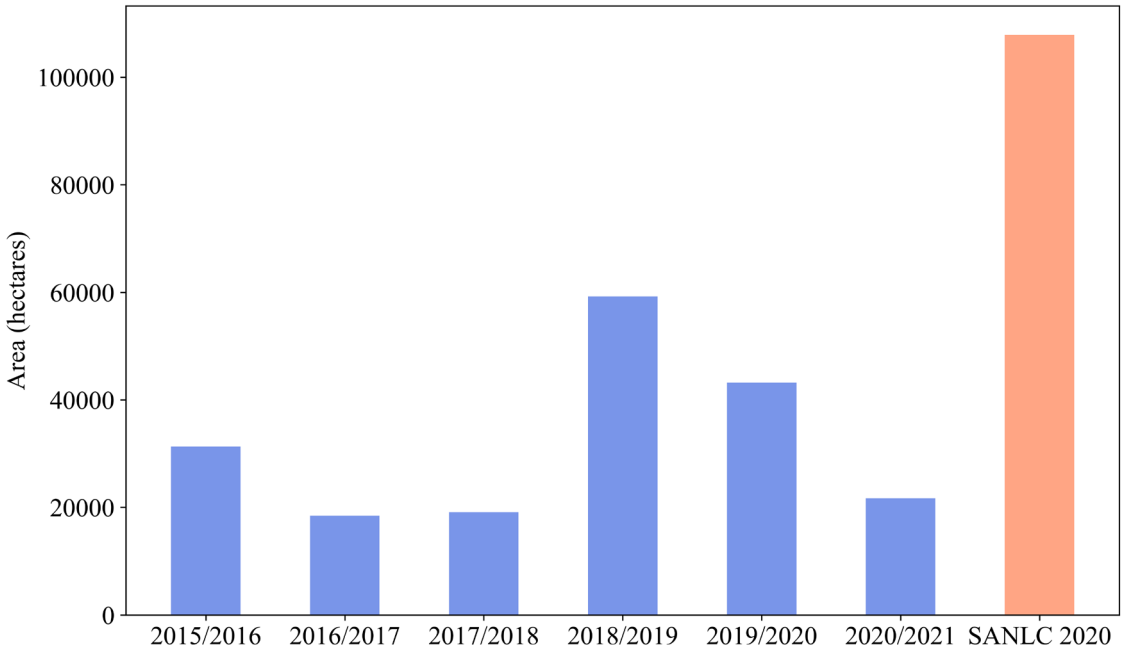

Figure 6. Unbiased area estimates of maize planted for the study area from 2015 to 2021 and the area classified by the SANLC (2020) as under subsistence/small-scale annual crops.

Figure 7 shows the changes in land cover for three regions in the Sekhukhune District from 2015 to 2021. The first region (see Figure 7a) depicts the changes in maize from 2015/2016 (Figure 7a1) to 2016/2017 (Figure 7a2). In 2016/2017, areas previously classified as under maize cultivation were then identified as bare soil, while those classified under the built-up class were then classified as bare soil or natural vegetation. This is an indication that a classification error occurred since it is unlikely for built-up areas to change into areas covered by natural vegetation. In the 2017/2018 (Figure 7b1) maize growing season, there were

considerably more bare soil areas interspersed with individual maize fields as opposed to the 2018/2019 growing season when maize crops predominated (Figure 7b1) in the second region (see Figure 7b). Lastly, from 2019/2020, the third region (see Figure 7c) showed a decline in the area under maize (Figure 7c1) which was subsequently accompanied by an increase in the areas under natural vegetation and bare soil during the 2020/2021 (Figure 7c2) growing season. There were further classification errors observed with areas classified as bare soil in 2019/2020 presenting as natural vegetation in 2020/2021. This could be due to the growth to some extent of natural vegetation in these areas since the bare soil class has similar spectral characteristics to those of the natural vegetation class.

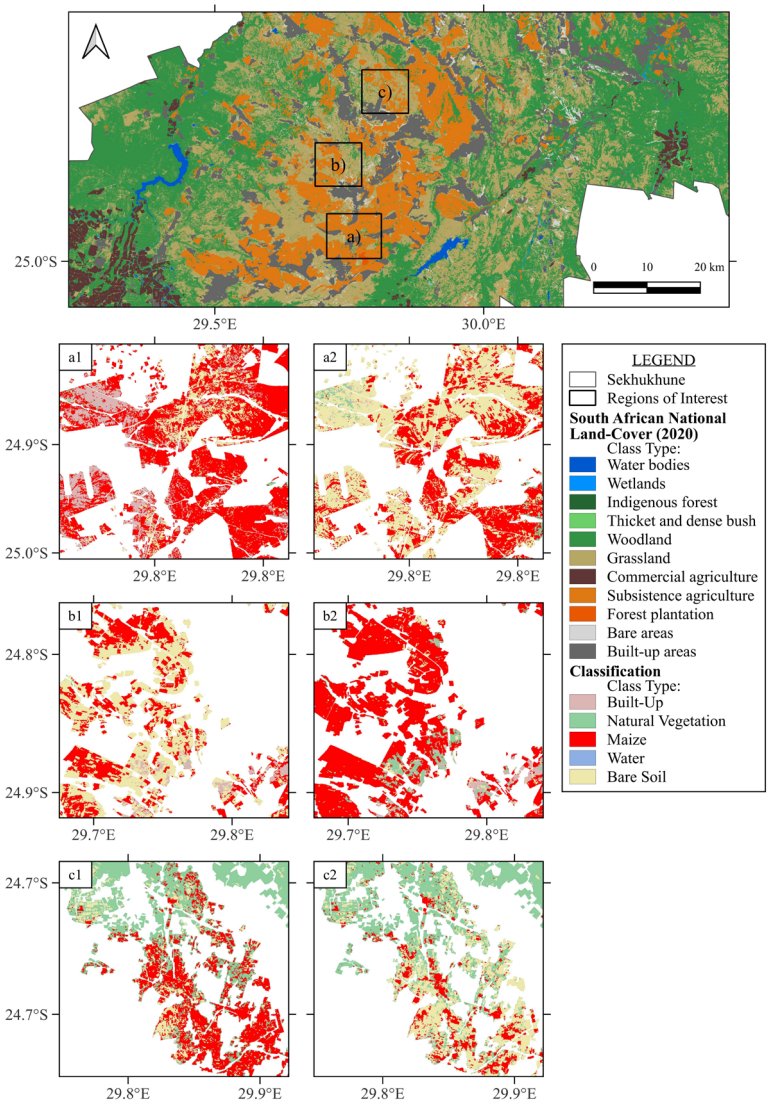

Figure 7. Classification maps using Model 24 for 2015/2016 (a1), 2016/2017 (a2), 2017/2018 (b1), 2018/2019 (b2), 2019/2020 (c1) and 2020/2021 (c2) for the Sekhukhune District study area.

4. Discussion

The main objective for the current study was to determine the best model for mapping the distribution of maize crops in Sekhukhune District over the 2015–2021 period. To achieve this, the study evaluated the performance of 24 different models (that incorporated Sentinel-1 monthly multi-temporal imagery and various ancillary datasets). The most effective models identified included those using monthly VH, VV and VV+VH polarization bands of Sentinel-1 and the principal component analysis (PCA)_VH monthly datasets. In addition to these, ancillary datasets, such as slope and elevation, monthly Sentinel-2 normalized difference vegetation index (NDVI) data, and Climate Hazards Group InfraRed Precipitation with Station (CHIRPS) rainfall data were also incorporated to improve the accuracy of the models. The results indicated that by integrating these Sentinel-1 composite images with all the ancillary datasets, the model for mapping smallholder maize crops and other land cover types in Sekhukhune District was the most accurate one to be produced.

The classification accuracy of models where only Sentinel-1 data were used produced overall accuracies (OAs) lower than 85% for Models 1, 7, 13 and 19. Furthermore, the average OAs for the models where only Sentinel-1 data were used were below 74% throughout the years under study (Table 3). Our study contradicted the findings of Chen et al. (2021), who reported that maize identification is mostly reliant on VV polarization. In their study, Chen et al. (2021) used monthly Sentinel-1 data, and included additional temporal variability data that significantly improved the accuracy of maize mapping. This indicates the importance of monthly composites when mapping areas under maize over the respective growing seasons. Similarly, Useya and Chen (2019) observed that accurate classifications of heterogeneous smallholder crops need more than just single-date Sentinel-1 images.

The most important variables for maize crop mapping in our study were Sentinel-2 NDVI, Sentinel-1 bands, and the slope and elevation datasets (Figure 5). Model 24 was the best-performing model for this study; this model was produced with dual-polarization (VV+VH) channels. The results agree with the findings of Li et al. (2019), namely, that these models and multi-polarization models outperform single-polarization models. The various Sentinel-1 bands are sensitive to maize growth at different periods in terms of crop height and phenology (Nasirzadehdizaji et al., 2019), and, as shown in Figure 3, there are temporal differences between the backscatter coefficients of the two channels (VH and VV). The models that included the Sentinel-1 PCA that derived from VH polarization bands, together with all the ancillary data, produced the second-highest average accuracy for all six growing seasons. The PCA method used in this study is a data reduction technique used on images. It transforms the multi-temporal backscatter values into components that provide more useful information (Mashaba-Munghemezulu et al., 2021b). Therefore, the PCA 1 and PCA 2 variables were able to produce variable importance scores like those of the Sentinel-2 NDVI variable. In this study,

combining optical and radar data proved essential, as each sensor proved to be beneficial to the mapping of smallholder maize. Other studies have shown that this is possible as each of these sensors can distinguish between various crop characteristics (Masiza et al., 2020). Finally, this research demonstrates that maize crop distribution can be reasonably mapped by using Sentinel-1 data combined with ancillary vegetation, climatic and topographic data.

Climatic variation is another important variable that influences crop growth. Therefore, the CHIRPS rainfall dataset was incorporated into this study. However, its incorporation served only slightly in improving the average accuracy over all six growing seasons (Table 3). The study by Omondi et al. (2021) investigated the performance of CHIRPS to detect rainfall events throughout the maize growing seasons. Their research found that over- and underestimations of rainfall were frequently made and that these influenced the crop growth stage. This could indicate that in terms of their contribution to the mapping of maize crops, rainfall data are not reliable.

The incorporation of Sentinel-2 NDVI imagery resulted in the most significant improvement in accuracy. The benefits accruing from combining Sentinel-2 NDVI data for modelling have been addressed by various studies in recent years (Mashaba-Munghemezulu et al., 2021a; Chakhar et al., 2021). Our results showed higher OAs when Sentinel-2 NDVI data were combined with Sentinel-1 data. These findings concur with those of Orynbaikyzy et al. (2020). The improved classification results found in our study can be attributed to the stable and smoother NDVI profiles for the maize crop as described by Ibrahim et al. (2021). These findings explain the better performance of the three models in our study, where NDVI, a vegetation index, was incorporated, possibly because such indices minimize the background noise, and focus instead on crop and vegetational cover (Jackson and Huete, 1991).

The observations in our study led to the conclusion that the incorporation of terrain data into the model further enhances mapping accuracies. The findings show greater OAs when ancillary datasets, including slope and elevation, were added. Gella et al. (2021) observed that crop mapping is hindered by complex landscapes and cropping systems and that incorporating slope and elevation data could, therefore, significantly improve the classification accuracy. Maize plant height is a defining characteristic that sets it apart from other crops, especially when slope and elevation are considered. Maize plants grown on steep slopes or at high elevations tend to be shorter than maize plants grown on even terrain and at lower elevations. For example, Mbugua et al. (2019) found that maize plants on the middle and upper slopes tend to be shorter on account of the lower soil moisture levels in those areas. Therefore, because these variables can impact the growth of maize crops over the course of a season, considerations of slope and elevation are justified (Tremblay et al., 2011).

By mapping the Sekhukhune District from 2015 to 2021, this study examined the distribution of the maize crop over time. Variations in the distribution of the maize crop were

observed throughout this period, with a significant increase observed in the 2018/2019 maize growing season, followed by a decline in the two subsequent growing seasons. According to Shikwambana and Malaza (2022), smallholder farmers in Limpopo, South Africa, are significantly affected by climate change. These authors have identified various risks that farmers face, such as crop loss owing to reduced rainfall and the increased occurrence of drought. As a result, farmers often resort to adapting their crops to various agricultural strategies (e.g., changing the planting dates), which could result in reduced harvests (Kom et al., 2020). To mitigate the impacts of the delayed onset of rains, the South African government should revise the cropping calendar accordingly. The timing of the distribution of farmer support should be adjusted to align with revised planting dates. Furthermore, new seed varieties that exhibit drought tolerance or a shift in focus toward cultivating more drought-tolerant crops should be explored. These recommendations are needed since changes in maize distribution have been shown to impact both the socioeconomic and food security situation of the rural community in Limpopo (Rankoana, 2022).

In recent years, the loss in smallholder maize production has been especially high, as seen in the decline in the area under maize identified for 2020/2021. This is most likely due to the impact of the COVID-19 pandemic, where reduced financial support from the government left smallholder farmers unable to meet their usual crop output standards (Nephawe et al., 2021). Furthermore, restricted travel/movement implemented during the COVID-19 pandemic prevented smallholder farmers from going into their fields to plant. By monitoring these changes in maize crop distribution, decision-makers can identify areas of potential food insecurity and take appropriate action to support smallholder farmers and ensure an adequate food supply for the local population.

Future projects should aim to provide spatial products for rural farmers. As such, these models should be explored for further development in other smallholder systems in South Africa. A major limitation of this study was that other vegetation indices, such as the soil-adjusted vegetation index (SAVI), the red-edge NDVI, or the radar vegetation index (RVI) should have been incorporated into this study. In the study by Letsoin et al. (2023), RVI computed from VH and VV+VH polarization bands could identify crop growth successfully. Such indices could contribute significantly to the success of classification models, which could then be incorporated into future models for mapping smallholder maize. Furthermore, the government and decision-makers could apply the concepts of the current research in areas where smallholder farmers are vulnerable to crop loss. The products of this research could also be used in decision-making and in promoting sustainable development in respect of smallholder communities.

5. Conclusion

The current study demonstrates that smallholder maize cropland can be accurately mapped using multi-temporal Sentinel-1 data in combination with landscape and climatic datasets. Monthly Sentinel-1 composites were created with VV and VH polarization bands and dual-polarization bands (VV+VH). Furthermore, a PCA_VH polarization composite was extracted for each of the six maize growing seasons. Each of the Sentinel-1 composites was combined with Sentinel-2 NDVI, slope, elevation and CHIRPS rainfall ancillary datasets to develop 24 composite models from 2015 to 2021. The models, either Sentinel-1 only or Sentinel-1 with one or two ancillary datasets, returned lower accuracy maps than was the case when all the datasets were combined. McNemar's test results showed that Model 6 produced classification results that concurred statistically with those for Models 5, 11, 12, 18, 23 and 24 for most of the growing seasons. For the six growing seasons, the average overall accuracy for these models was above 85%. Model 24 produced the most favourable results in that it was able to distinguish more accurately between smallholder maize and other land cover types. The maize area estimates presented in this model show that 2018/2019 had the largest area (59 240.84 ha) under maize in the study area and compared well with the lowest (18 462.51 ha) for the same area in 2016/2017. The findings of this research study would be ideal for developing management plans and assisting rural farmers in providing spatial data for decision-making. The outcome of this study will be especially useful in the long-term multi-year planning and regional scale mapping of smallholder crop distribution.

6. Acknowledgements

The authors express their sincere gratitude to the Agricultural Research Council (ARC), the University of Pretoria, the National Research Foundation (NRF), and the Agricultural Sector Education Training Authority (AgriSETA) for their continual support during this project. This work was supported by the ARC under Grant P070000198 and by the NRF under Grant TTK23030981636.

7. References

Abubakar, G. A., Wang, K., Koko, A. F., Husseini, M. I., Shuka, K. A. M., Deng, J. & Gan, M. 2023. Mapping maize cropland and land cover in a semi-arid region in Northern Nigeria using machine learning and Google Earth Engine. *Remote Sensing,* 15**,** 2835.

Abubakar, G. A., Wang, K., Shahtahamssebi, A., Xue, X., Belete, M., Gudo, A. J. A., Mohamed Shuka, K. A. & Gan, M. 2020. Mapping maize fields by using multi-temporal Sentinel-1A and Sentinel-2A images in Makarfi, Northern Nigeria, Africa. *Sustainability,* 12**,** 2539.

Aduvukha, G. R., Abdel-Rahman, E. M., Sichangi, A. W., Makokha, G. O., Landmann, T., Mudereri, B. T., Tonnang, H. E. & Dubois, T. 2021. Cropping pattern mapping in an agro-natural heterogeneous landscape using Sentinel-2 and Sentinel-1 satellite datasets. *Agriculture,* 11**,** 530.

Amani, M., Ghorbanian, A., Ahmadi, S. A., Kakooei, M., Moghimi, A., Mirmazloumi, S. M., Moghaddam, S. H. A., Mahdavi, S., Ghahremanloo, M. & Parsian, S. 2020. Google Earth Engine cloud-computing platform for remote sensing big data applications: A comprehensive review. *IEEE Journal of Selected Topics in Applied Earth Observations and Remote Sensing,* 13**,** 5326-5350.

Andrade, R., Urioste, S., Rivera, T., Schiek, B., Nyakundi, F., Vergara, J., Mwanzia, L., Loaiza, K. & Gonzalez, C. 2021. Where is my crop? Data-driven initiatives to support integrated multi-stakeholder agricultural decisions. *Frontiers in Sustainable Food Systems,* 5**,** 737528.

Arslan, İ., Topakcı, M. & Demir, N. 2022. Monitoring maize growth and calculating plant heights with Synthetic Aperture Radar (SAR) and optical satellite images. *Agriculture,* 12**,** 800.

Azzari, G., Jain, S., Jeffries, G., Kilic, T. & Murray, S. 2021. Understanding the requirements for surveys to support satellite-based crop-type mapping: Evidence from sub-Saharan Africa. *Remote Sensing,* 13**,** 4749.

Bosc, P.-M., Berdegué, J., Goïta, M., van der Ploeg, J. D., Sekine, K. & Zhang, L. 2013. *Investing in smallholder agriculture for food security*, HLPE.

Breiman, L. 2001. Random Forests. *Machine Learning,* 45**,** 5–32.

Brewer, K., Clulow, A., Sibanda, M., Gokool, S., Naiken, V. & Mabhaudhi, T. 2022. Predicting the chlorophyll content of maize over phenotyping as a proxy for crop health in smallholder farming systems. *Remote Sensing,* 14**,** 518.

Chakhar, A., Hernández-López, D., Ballesteros, R. & Moreno, M. A. 2021. Improving the accuracy of multiple algorithms for crop classification by integrating Sentinel-1 observations with Sentinel-2 data. *Remote Sensing,* 13**,** 243.

Chen, Y., Hou, J., Huang, C., Zhang, Y. & Li, X. 2021. Mapping maize area in a heterogeneous agricultural landscape with multi-temporal Sentinel-1 and Sentinel-2 images based on random forest. *Remote Sensing,* 13**,** 2988.

Chivasa, W., Mutanga, O. & Biradar, C. 2017. Application of remote sensing in estimating maize grain yield in heterogeneous African agricultural landscapes: a review. *International Journal of Remote Sensing,* 38**,** 6816–6845.

Congalton, R. G. & Green, K. 2019. *Assessing the accuracy of remotely sensed data: principles and practices*, CRC press.

Department of Forestry, F. a. t. E. 2020. South African National Land Cover

Dlamini, L., Crespo, O., van Dam, J. & Kooistra, L. 2023. A global systematic review of improving crop model estimations by assimilating remote sensing data: implications for small-scale agricultural systems. *Remote Sensing,* 15**,** 4066.

Drimie, S., Germishuyse, T., Rademeyer, L. & Schwabe, C. 2009. Agricultural production in Greater Sekhukhune: the future for food security in a poverty node of South Africa? *Agrekon,* 48**,** 245–275.

European Space Agency. 2024a. *Sentinel-1 Products* [Online]. Available from: https://sentiwiki.copernicus.eu/web/s1-products [Accessed: 2 June 2024].

European Space Agency. 2024b. *Sentinel-1 Toolbox* [Online]. Available from: https://sentiwiki.copernicus.eu/web/sentinels-toolboxes [Accessed: 2 June 2024].

Farr, T. G., Rosen, P. A., Caro, E., Crippen, R., Duren, R., Hensley, S., Kobrick, M., Paller, M., Rodriguez, E. & Roth, L. 2007. The shuttle radar topography mission. *Reviews of Geophysics,* 45.

Filipponi, F. 2019 Published. Sentinel-1 GRD preprocessing workflow. In: *Proceedings*. MDPI, 11.

Funk, C., Peterson, P., Landsfeld, M., Pedreros, D., Verdin, J., Shukla, S., Husak, G., Rowland, J., Harrison, L. & Hoell, A. 2015. The climate hazards infrared precipitation with stations—a new environmental record for monitoring extremes. *Scientific Data,* 2**,** 1-21.

Gella, G. W., Bijker, W. & Belgiu, M. 2021. Mapping crop types in complex farming areas using SAR imagery with dynamic time warping. *ISPRS Journal of Photogrammetry and Remote Sensing,* 175**,** 171–183.

Geological Survey 1986. 2428 Nylstroom, 1:250 000 Geological Series. Department of Mineral and Energy Affairs, Pretoria.

Hazell, P., Spencer, D. & Gulati, A. 2002 Published. The future of agriculture in Sub-Saharan Africa and South Asia: Whither the small farm? In: *Sustainable food security for all by 2020: Proceedings of an International Conference, Bonn, Germany, 4-6 September, 2001*. International Food Policy Research Institute, 107–114.

Hegarty-Craver, M., Polly, J., O'Neil, M., Ujeneza, N., Rineer, J., Beach, R. H., Lapidus, D. & Temple, D. S. 2020. Remote crop mapping at scale: Using satellite imagery and UAV-acquired data as ground truth. *Remote Sensing,* 12**,** 1984.

Ibrahim, E. S., Rufin, P., Nill, L., Kamali, B., Nendel, C. & Hostert, P. 2021. Mapping crop types and cropping systems in Nigeria with Sentinel-2 imagery. *Remote Sensing,* 13**,** 3523.

International Fund for Agricultural Development, U. 2013. Smallholders, food security and the environment. *Rome: International Fund for Agricultural Development,* 29.

Jackson, R. D. & Huete, A. R. 1991. Interpreting vegetation indices. *Preventive Veterinary Medicine,* 11**,** 185–200.

Jin, Z., Azzari, G., You, C., Di Tommaso, S., Aston, S., Burke, M. & Lobell, D. B. 2019. Smallholder maize area and yield mapping at national scales with Google Earth Engine. *Remote Sensing of the Environment,* 228**,** 115–128.

Jolliffe, I. T. 2002. *Principal component analysis,* New York, Springer.

Kebede, E. 2020. Grain legume production and productivity in Ethiopian smallholder agricultural system, contribution to livelihoods and the way forward. *Cogent Food & Agriculture,* 6**,** 1722353.

Kerner, H., Nakalembe, C. & Becker-Reshef, I. 2020a. Field-level crop type classification with k nearest neighbors: a baseline for a new Kenya smallholder dataset. *arXiv arXiv:2004.03023*.

Kerner, H., Tseng, G., Becker-Reshef, I., Nakalembe, C., Barker, B., Munshell, B., Paliyam, M. & Hosseini, M. 2020b. Rapid response crop maps in data sparse regions. *arXiv arXiv:2006.16866*.

Kibret, K. S., Marohn, C. & Cadisch, G. 2020. Use of MODIS EVI to map crop phenology, identify cropping systems, detect land-use change and drought risk in Ethiopia – an application of Google Earth Engine. *European Journal of Remote Sensing,* 53**,** 176–191.

Kleynhans, C., Thirion, C. & Moolman, J. 2005. A Level I river ecoregion classification system for South Africa, Lesotho and Swaziland. *Pretoria: Department of Water Affaris and Forestry*.

Kom, Z., Nethengwe, N., Mpandeli, N. & Chikoore, H. 2020. Determinants of small-scale farmers' choices and adaptive strategies in response to climatic shocks in Vhembe District, South Africa. *GeoJournal***,** 1–24.

Letsoin, S. M. A., Purwestri, R. C., Perdana, M. C., Hnizdil, P. & Herak, D. 2023. Monitoring of paddy and maize fields using Sentinel-1 SAR data and NGB Images: a case study in Papua, Indonesia. *Processes,* 11**,** 647.

Li, L., Kong, Q., Wang, P., Xun, L., Wang, L., Xu, L. & Zhao, Z. 2019. Precise identification of maize in the North China Plain based on Sentinel-1A SAR time series data. *International Journal of Remote Sensing,* 40**,** 1996-2013.

Li, W., Niu, Z., Wang, C., Huang, W., Chen, H., Gao, S., Li, D. & Muhammad, S. 2015. Combined use of airborne LiDAR and satellite GF-1 data to estimate leaf area index, height, and aboveground biomass of maize during the peak growing season. *IEEE Journal of Selected Topics in Applied Earth Observations and Remote Sensing,* 8**,** 4489-4501.

Li, Y., Ma, J. & Zhang, Y. 2021. Image retrieval from remote sensing big data: A survey. *Information Fusion,* 67**,** 94-115.

Liepa, A., Thiel, M., Taubenböck, H., Steffan-Dewenter, I., Abu, I.-O., Dhillon, M. S., Otte, I., Otim, M. H., Lutaakome, M. & Meinhof, D. 2024. Harmonized NDVI time-series from Landsat and Sentinel-2 reveal phenological patterns of diverse small-scale cropping systems in East Africa. *Remote Sensing Applications: Society and Environment***,** 101230.

Louis, J., Pflug, B., Main-Knorn, M., Debaecker, V., Mueller-Wilm, U., Iannone, R. Q., Cadau, E. G., Boccia, V. & Gascon, F. 2019 Published. Sentinel-2 global surface reflectance level-2A product generated with Sen2Cor. In: *IGARSS 2019-2019 IEEE International Geoscience and Remote Sensing Symposium*. IEEE, 8522-8525.

Luo, C., Qi, B., Liu, H., Guo, D., Lu, L., Fu, Q. & Shao, Y. 2021. Using time series Sentinel-1 images for object-oriented crop classification in Google Earth Engine. *Remote Sensing,* 13**,** 561.

Mahlayeye, M., Darvishzadeh, R. & Nelson, A. 2022. Cropping patterns of annual crops: a remote sensing review. *Remote Sensing,* 14**,** 2404.

Main-Knorn, M., Pflug, B., Louis, J., Debaecker, V., Müller-Wilm, U. & Gascon, F. 2017 Published. Sen2Cor for Sentinel-2. In: *Image and Signal Processing for Remote Sensing XXIII*. SPIE, 37-48.

Masekoameng, M. & Molotja, M. 2016. The impacts of climate change on household food security: the case of Mogaladi village in Sekhukhune district, South Africa. *Indilinga African Journal of Indigenous Knowledge Systems,* 15**,** 49-70.

Mashaba-Munghemezulu, Z., Chirima, G. J. & Munghemezulu, C. 2021a. Delineating smallholder maize farms from Sentinel-1 coupled with Sentinel-2 data, using machine learning. *Sustainability,* 13**,** 4728.

Mashaba-Munghemezulu, Z., Chirima, G. J. & Munghemezulu, C. 2021b. Mapping smallholder maize farms using multi-temporal Sentinel-1 data in support of the Sustainable Development Goals. *Remote Sensing,* 13**,** 1666.

Masiza, W., Chirima, J. G., Hamandawana, H., Kalumba, A. M. & Magagula, H. B. 2022a. Do satellite data correlate with *in situ* rainfall and smallholder crop yields? Implications for crop insurance. *Sustainability,* 14**,** 1670.

Masiza, W., Chirima, J. G., Hamandawana, H., Kalumba, A. M. & Magagula, H. B. 2022b. A proposed satellite-based crop insurance system for smallholder maize farming. *Remote Sensing,* 14**,** 1512.

Masiza, W., Chirima, J. G., Hamandawana, H. & Pillay, R. 2020. Enhanced mapping of a smallholder crop farming landscape through image fusion and model stacking. *International Journal of Remote Sensing,* 41**,** 8739-8756.

Mbhenyane, X. G., Tambe, B., Phooko-Rabodiba, D. & Nesamvuni, C. 2020. Dietary pattern, household hunger, coping strategies and nutritional status of children in Sekhukhune District of Limpopo Province, South Africa. *African Journal of Food, Agriculture, Nutrition and Development,* 20**,** 15821-15836.

Mbugua, H., Baaru, M. & Gachene, C. 2019. Soil moisture variability effects on maize crop performance along a toposequence of a terraced vertisol in Machakos, Kenya. *Journal of Soil Science and Environmental Management,* 10**,** 21-28.

Mokgolo, M. & Mzezewa, J. 2022. Baseline study of soil nutrient status in smallholder farms in Limpopo province of South Africa. *South African Journal of Agricultural Extension,* 50**,** 51-65.

Montelpare, W. & McPherson, M. 2000. Client-side processing on the InterNet: computing the McNemar test of symmetry and the kappa statistic for paired response data. *The International Electronic Journal for Health Education,* 3**,** 253-271.

Mpakairi, K. S., Dube, T., Sibanda, M. & Mutanga, O. 2023. Fine-scale characterization of irrigated and rainfed croplands at national scale using multi-source data, random forest, and deep learning algorithms. *ISPRS Journal of Photogrammetry and Remote Sensing,* 204**,** 117-130.

Mpandeli, S., Nesamvuni, E. & Maponya, P. 2015. Adapting to the impacts of drought by smallholder farmers in Sekhukhune District in Limpopo Province, South Africa. *Journal of Agricultural Science,* 7**,** 115.

Mudhara, M. & Senzanje, A. 2020. Assessment of policies and strategies for the governance of smallholder irrigation farming in Kwazulu-Natal province, South Africa. *Water Research Commission*.

Nasirzadehdizaji, R., Balik Sanli, F., Abdikan, S., Cakir, Z., Sekertekin, A. & Ustuner, M. 2019. Sensitivity analysis of multi-temporal Sentinel-1 SAR parameters to crop height and canopy coverage. *Applied Sciences,* 9**,** 655.

Nasirzadehdizaji, R., Cakir, Z., Sanli, F. B., Abdikan, S., Pepe, A. & Calo, F. 2021. Sentinel-1 interferometric coherence and backscattering analysis for crop monitoring. *Computers and Electronics in Agriculture,* 185**,** 106118.

Nephawe, N., Mwale, M., Zuwarimwe, J. & Kativhu, S. 2021. Water-related challenges in crop production: Insights from under-resourced small-scale farmers in Limpopo Province of South Africa. *African Renaissance,* 18**,** 1744-2532.

Ni, R., Zhu, X., Lei, Y., Li, X., Dong, W., Zhang, C., Chen, T., Mburu, D. M. & Hu, C. 2022. Effectiveness of common preprocessing methods of time series for monitoring crop distribution in Kenya. *Agriculture,* 12**,** 79.

Nzuza, P., Ramoelo, A., Odindi, J., Mwenge Kahinda, J.-M. & Lindeque, L. 2022. A triangulation approach for assessing and mapping land degradation in the Lepellane catchment of the greater Sekhukhune District, South Africa. *South African Geographical Journal,* 104**,** 514-538.

Olofsson, P., Foody, G. M., Stehman, S. V. & Woodcock, C. E. 2013. Making better use of accuracy data in land change studies: Estimating accuracy and area and quantifying uncertainty using stratified estimation. *Remote Sensing of the Environment,* 129**,** 122-131.

Omondi, C. K., Rientjes, T. H., Booij, M. J. & Nelson, A. D. 2021. Satellite rainfall bias assessment for crop growth simulation–a case study of maize growth in Kenya. *Agricultural Water Management,* 258**,** 107204.

Orynbaikyzy, A., Gessner, U. & Conrad, C. 2022. Spatial transferability of random forest models for crop type classification using Sentinel-1 and Sentinel-2. *Remote Sensing,* 14**,** 1493.

Orynbaikyzy, A., Gessner, U., Mack, B. & Conrad, C. 2020. Crop type classification using fusion of Sentinel-1 and Sentinel-2 data: Assessing the impact of feature selection, optical data availability, and parcel sizes on the accuracies. *Remote Sensing,* 12**,** 2779.

Rankoana, S. A. 2022. Indigenous knowledge and innovative practices to cope with impacts of climate change on small-scale farming in Limpopo Province, South Africa. *International Journal of Climate Change Strategies and Management*.

Ren, T., Xu, H., Cai, X., Yu, S. & Qi, J. 2022. Smallholder crop type mapping and rotation monitoring in mountainous areas with Sentinel-1/2 imagery. *Remote Sensing,* 14**,** 566.

Shiferaw, B., Prasanna, B. M., Hellin, J. & Bänziger, M. 2011. Crops that feed the World Six. Past successes and future challenges to the role played by maize in global food security. *Food Security,* 3**,** 307-327.

Shikwambana, S. & Malaza, N. 2022. Enhancing the resilience and adaptive capacity of smallholder farmers to drought in the Limpopo Province, South Africa. *Conservation,* 2**,** 435-449.

Shuai, G., Zhang, J., Basso, B., Pan, Y., Zhu, X., Zhu, S. & Liu, H. 2019. Multi-temporal RADARSAT-2 polarimetric SAR for maize mapping supported by segmentations from high-resolution optical images. *International Journal of Applied Earth Observation and Geoinformation,* 74**,** 1-15.

Statistics South Africa. 2011. *Statistics South Africa, Census 2011* [Online]. Available from: https://www.statssa.gov.za/ [Accessed: 6 June 2024].

Stuch, B., Alcamo, J. & Schaldach, R. 2021. Projected climate change impacts on mean and year-to-year variability of yield of key smallholder crops in Sub-Saharan Africa. *Climate and Development,* 13**,** 268-282.

Tamiminia, H., Salehi, B., Mahdianpari, M., Quackenbush, L., Adeli, S. & Brisco, B. 2020. Google Earth Engine for geo-big data applications: a meta-analysis and systematic review. *ISPRS Journal of Photogrammetry and Remote Sensing,* 164**,** 152-170.

Tremblay, N., Bouroubi, M. Y., Vigneault, P. & Bélec, C. 2011. Guidelines for in-season nitrogen application for maize (*Zea mays* L.) based on soil and terrain properties. *Field Crops Research,* 122**,** 273-283.

Trivedi, M. B., Marshall, M., Estes, L., de Bie, C., Chang, L. & Nelson, A. 2023. Cropland mapping in tropical smallholder systems with seasonally stratified Sentinel-1 and Sentinel-2 spectral and textural features. *Remote Sensing,* 15**,** 3014.

Useya, J. & Chen, S. 2019. Exploring the potential of mapping cropping patterns on smallholder scale croplands using Sentinel-1 SAR data. *Chinese Geographical Science,* 29**,** 626-639.

Vogels, M. F., De Jong, S. M., Sterk, G., Douma, H. & Addink, E. A. 2019. Spatio-temporal patterns of smallholder irrigated agriculture in the Horn of Africa using GEOBIA and Sentinel-2 imagery. *Remote Sensing,* 11**,** 143.

Vuolo, F., Neuwirth, M., Immitzer, M., Atzberger, C. & Ng, W.-T. 2018. How much does multi-temporal Sentinel-2 data improve crop-type classification? *International Journal of Applied Earth Observation and Geoinformation,* 72**,** 122-130.

Wen, Y., Li, X., Mu, H., Zhong, L., Chen, H., Zeng, Y., Miao, S., Su, W., Gong, P. & Li, B. 2022. Mapping corn dynamics using limited but representative samples with adaptive strategies. *ISPRS Journal of Photogrammetry and Remote Sensing,* 190**,** 252-266.

Zerssa, G., Feyssa, D., Kim, D.-G. & Eichler-Löbermann, B. 2021. Challenges of smallholder farming in Ethiopia and opportunities by adopting climate-smart agriculture. *Agriculture,* 11**,** 192.